Spurious-free dynamic range improvement in a photonic time-stretched analog-to-digital converter based on third-order predistortion

Boyu Xu, Wulue Lv, Jiamu Ye, Jinhai Zhou, Xiaofeng Jin,* Xianmin Zhang, Hao Chi, and Shilie Zheng

Department of Information Science and Electronic Engineering, Zhejiang University, Hangzhou 310027, China
**Corresponding author: jinxf00@zju.edu.cn*

Received April 2, 2014; revised May 16, 2014; accepted May 17, 2014;
posted May 20, 2014 (Doc. ID 209358); published August 1, 2014

Spurious-free dynamic range (SFDR) limited by intermodulation distortions is a usually accepted measure for dynamic performance of a photonic time-stretched analog-to-digital converter (ADC). In this paper, SFDR improvement in a photonic time-stretched ADC based on third-order predistortion is proposed. The third-order predistortion is achieved optically within an integrated dual-parallel Mach–Zehnder modulator (DPMZM). The mechanism of SFDR improvement with third-order predistortion in the DPMZM is theoretically analyzed. Compared with a conventional scheme without predistortion, the experimental results show that the SFDR improvement of ~26 dB in the proposed scheme is proved.

OCIS codes: (060.2360) Fiber optics links and subsystems; (070.4340) Nonlinear optical signal processing; (070.4560) Data processing by optical means.
http://dx.doi.org/10.1364/PRJ.2.000097

1. INTRODUCTION

Analog-to-digital converters (ADCs), which convert continuous-time signals to digital form, are among the keys to the success of signal processing systems, including medical imaging, sonar, radar, and telecommunications [1]. However, the performance of the conventional electronic ADCs is limited by the input-referred noise, aperture jitter, and comparator ambiguity [2]. In order to overcome the bottleneck of electronic ADCs, photonic ADCs that use photonics in the digitalization process have been proposed in recent years [3]. Compared with electronic-based ADCs, the photonic method enjoys the advantages of low loss, high time-bandwidth product, and immunity to electromagnetic interference [4]. Photonic ADCs can be divided into several classes depending on whether the sampling and quantization are performed in the photonic domain. Among those, the photonic time-stretched ADC with sampling and quantization performed in the electronic domain can use photonic methods to enhance the performance of the electronic ADC. The enhancements include an increase in the sampling rate and the input bandwidth, reduction in the digitizer sampling jitter noise, and interchannel mismatch errors [5]. Meanwhile, one of the disadvantages of the photonic time-stretched ADC is that the photonic processing of the electronic signal usually requires a Mach–Zehnder modulator (MZM) to achieve electro-optic conversion. However, the transfer function of the MZM generally has nonlinear response, within which nonlinear distortions such as harmonic distortions and intermodulation distortions (IMDs) are induced into the system. These undesired components will reduce the performance of the electronic ADC, such as the reduction of the spurious-free dynamic range (SFDR), which is a usually accepted measure for the dynamic performance of an ADC [1]. To cancel the even-order harmonics and IMDs in the photonic time-stretched ADC, differential pull–push modulation was proposed in [6]. However, the amplitude and phase mismatches will weaken the effectiveness of the differential operation by reducing the distortion rejection ratio (DDR) [7]. Meanwhile, in most cases, the third-order IMD (IMD3) is the largest limitation of the SFDR since IMD3 always exists in the spectrum of interest and is difficult to filter out.

In this paper, we propose a new scheme to improve the IMD3-determined SFDR of the photonic time-stretched ADC based on the third-order predistortion. The technique of high-order predistortion has been widely used to achieve linearization in both electronics and photonics [8–10]. In our scheme, the technique of third-order predistortion is adopted by employing a dual-parallel MZM (DPMZM) to generate the predistorted IMD3 components. By tuning the bias voltages of the DPMZM to the specific points, the third nonlinear distortions caused by intermodulation in the system can be largely reduced by the generated predistorted IMD3 within the DPMZM. The proposed approach of SFDR improvement is effective and easy to realize.

2. PRINCIPLE OF OPERATION

A photonic time-stretched ADC is usually composed of two parts, the photonic time-stretched preprocessor, which is used to stretch the input radio frequency (RF) signal in the time domain, and an electronic ADC, as shown in Fig. 1. First, an optical pulse generated by the super-continuum source is chirped and broadened after propagating thorough the first dispersive medium, which induces the effects of group-velocity dispersion (GVD). Then the chirped optical pulse will take the envelope of the input RF signal after modulation. The envelope of the optical pulse will be further broadened when

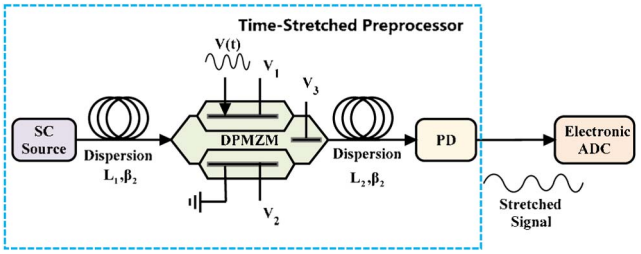

Fig. 1. Schematic illustration of the proposed photonic time-stretched ADC based on third-order predistortion (SC, supercontinuum).

the pulse propagates through the second dispersive medium. Finally, through the photo-detector (PD), we can get a stretched RF signal, and compared with the original one, it is proved that the stretched factor M can be written as $M = (D_1 + D_2)/D_1$ [5], where D_1 and D_2 represent the total dispersions of the first and second dispersive media. In order to understand the principle of our linearized scheme based on third-order predistortion, a theoretical derivation is given as follows.

Assume that the optical pulse is a Gaussian-shaped pulse generated by the super-continuum optical source. In the frequency domain, the electric field of the optical pulse can be written as [11]

$$E_1(\omega) = E_0(2\pi T_0^2)^{1/2} \exp\left(\frac{-\omega^2 T_0^2}{2}\right), \tag{1}$$

where E_0 is the pulse amplitude and T_0 is the pulse half-width (at a $1/e$-intensity point). After propagating through the first dispersive medium, the optical pulse becomes broadened and chirped. Supposing higher-order dispersion is much smaller, only first-order dispersion is taken into consideration, and the electric field in the frequency domain becomes

$$E_2(\omega) = E_1(\omega) \exp\left(\frac{jL_1\beta_2\omega^2}{2}\right), \tag{2}$$

where L_1 is the length of the first dispersive medium, and β_2 is the GVD parameter.

Then the chirped optical pulse is sent to an X-cut integrated DPMZM, which can be seen as a combination of three sub-MZMs: an upper MZM, a lower MZM, and a main MZM. The DPMZM is used to modulate the input RF signal onto the chirped optical pulse and predistort the IMD3 component. Within the DPMZM, the RF signal is connected to the input of the upper MZM, the RF input of the lower MZM is shorted, and three sub-MZMs are biased at V_1, V_2, and V_3, respectively. The electric field of the output of the DPMZM in the time domain can be represented as

$$E_3(t) = \frac{E_2(t)}{2}\left[\cos\frac{\varphi_1(t)}{2} e^{j\varphi_3/2} + \cos\frac{\varphi_2}{2} e^{-j\varphi_3/2}\right], \tag{3}$$

where $E_2(t)$ is the inverse Fourier transform of $E_2(\omega)$, $\varphi_1(t) = \varphi_1 + V(t)$, $\varphi_i = \pi V_i/V_{\pi i}$ $(i = 1, 2, 3)$ are the phase differences between two arms of each sub-MZM, and $V_{\pi i}$ $(i = 1, 2, 3)$ is the half-wave voltage.

Then the output of the DPMZM passes through the second dispersive medium, which has a same GVD parameter with the first dispersive medium, and the electric field in the frequency domain becomes

$$E_4(\omega) = E_3(\omega) \exp\left(\frac{jL_2\beta_2\omega^2}{2}\right), \tag{4}$$

where L_2 is the length of the second dispersive medium.

Finally, the stretched optical pulse is sent to a PD to accomplish photoelectric conversion. The intensity of the current $I(t)$ is proportional to the square of the electric field, which can be written as

$$I(t) \propto |E_4(t)|^2. \tag{5}$$

In order to analyze the third-order IMD components, a two-tone RF signal is input to drive the DMPZM,

$$V(t) = m[\cos(\omega_1 t) + \cos(\omega_2 t)], \tag{6}$$

where $m = \pi V_E/V_{\pi 1}$ is the modulation index, and V_E is the amplitude of the RF signal.

By applying a Bessel expansion to Eq. (3), the third-order component can be written as

$$\mathrm{IMD3} = E_2(t) e^{j\varphi_3/2} J_1\left(\frac{m}{2}\right) J_2\left(\frac{m}{2}\right) \sin\left(\frac{\varphi_1}{2}\right) \cos(2\omega_2 t \pm \omega_1 t), \tag{7}$$

where J_n represents the nth-order Bessel function of the first kind. As shown in Eq. (7), the amplitude and the phase of the IMD3 components are relative to φ_1 and φ_3. So by tuning the bias voltages, the predistortion of the IMD3 components can be controlled.

In this case, Eq. (5) can be expanded to

$$I(t) \propto I_{\mathrm{env}}(t)\left\{\Gamma_0 + \Gamma_1\left[\cos\left(\frac{\omega_1 t}{M}\right) + \cos\left(\frac{\omega_2 t}{M}\right)\right] + \Gamma_3\left[\cos\left(\frac{2\omega_1 t \pm \omega_2 t}{M}\right) + \cos\left(\frac{2\omega_2 t \pm \omega_1 t}{M}\right)\right]\cdots\right\}, \tag{8}$$

where $I_{\mathrm{env}}(t)$ is the envelope of the detected current, Γ_i $(i = 0, 1, 3)$ represents the coefficients of the direct current (DC), fundamental, and IMD3 components, respectively, and $M = (L_1 + L_2)/L_1$.

Ignoring the high-order components, the IMD3 can be divided into two parts; one is the beating between the carrier and the IMD3 components generated by the modulation, and the other is the beating between fundamental and second harmonics thorough PD. So the coefficient of the IMD3 is given by

$$\Gamma_3 = K\left[\begin{array}{l} J_0\left(\frac{m}{2}\right) J_1\left(\frac{m}{2}\right)^2 \cos\left(\frac{\varphi_1}{2}\right) \\ +J_2\left(\frac{m}{2}\right)\left(2J_0\left(\frac{m}{2}\right)^2 \cos\left(\frac{\varphi_1}{2}\right) + \cos\left(\frac{\varphi_2}{2}\right)\cos(\varphi_3)\right) \end{array}\right], \tag{9}$$

where $K = 4\sin(\varphi_1/2)\cos(\varphi_D)\, J_1(m/2)$, and $\cos(\varphi_D)$ is the power penalty induced by dispersion.

By expanding Eq. (9) in series and ignoring the high-order term, Γ_3 can be written as

$$\Gamma_3 = K\left[\frac{m^2}{32}\left(4\cos\left(\frac{\varphi_1}{2}\right)+\cos\left(\frac{\varphi_2}{2}\right)\cos(\varphi_3)\right) -\frac{m^4}{64}\cos\left(\frac{\varphi_1}{2}\right)+O(m^4)\right]. \quad (10)$$

In this condition, if the biases of the DPMZM satisfy

$$4\cos\left(\frac{\varphi_1}{2}\right)+\cos\left(\frac{\varphi_2}{2}\right)\cos(\varphi_3)=0, \quad (11)$$

the first term of the Γ_3 can be canceled, which means that the two components of the IMD3 are predistorted to have equal intensity but opposite phase, so that the IMD3 of the photonic time-stretched ADC can be largely reduced.

It should be noted that a perfect third-order predistortion may enhance the even-order harmonics and third-order harmonics, which can reduce the performance of the scheme. In most cases, these harmonics are far from the spectrum of our interest, and can be easily removed by a filter. In some cases, the frequency selectivity of the photonic time-stretched preprocessor will weaken the enhancement and make these components have little influence on the improvement of SFDR. Since the transfer function of the photonic time-stretched preprocessor can be written as [5]

$$H=(\cos(2\pi^2\beta_2 L_2 f^2/M))^2, \quad (12)$$

if the frequency of the input signal is known in advance, for example, in digital communications or a radar system, the parameter of the optical link can be adjusted to suppress certain harmonics.

3. EXPERIMENTS AND RESULTS

Figure 2 shows the experimental setup of the proposed photonic time-stretched system based on the third-order predistortion. As shown, a mode-locked laser (MLL), used as a super-continuum optical source, generates the optical pulse at a repetition rate of 25 MHz. The spectrum of the pulse with width of ~300 fs has a range of 12 nm, and it is centered at the wavelength of 1546 nm. The ultrashort pulse is then sent to the dispersion compensating fiber (DCF) with the dispersion coefficient D_1 of –58.8 ps/nm, to generate a chirped and broadened optical waveform of which the half-width is ~600 ps. Two different frequency RF signals generated by two oscillators are set to $f_1 = 9400$ MHz, and $f_2 = 9500$ MHz. Then the two RF signals are combined by a 3 dB coupler to become a two-tone RF signal. The two-tone RF signal and the chirped optical pulse are connected to the DPMZM as shown in Fig. 1. To generate the proper predistorted IMD3 component, the specifically designed biases of the DPMZM are set to $V_1 = 7.6$ V, $V_2 = 5.6$ V, and $V_3 = 2.3$ V, respectively, to satisfy Eq. (11) in the last section. The output of the DPMZM then propagates through the DCF with a dispersion coefficient D_2 of ~ – 1377 ps/nm. The stretch factor M of our proposed photonic time-stretched system can be calculated to be $M = (D_1 + D_2)/D_1 = 24.5$.

And the photoelectric convention is achieved by a PD with a bandwidth of 880 MHz. In order to analyze the SFDR of the photonic time-stretched ADC, the stretched electrical signal is sent to a spectrum analyzer instead of an electronic ADC.

A comparison with a conventional scheme without predistortion that uses a common MZM biased at the quadrature point is performed. The RF signal input to the modulator has a power level of 20 dBm, and the optical power input to the PD is about 3 dBm. The frequency of the RF signal f_2 is changed from 9500 to 388.83 MHz; i.e., the measured stretched factor M is calculated to be 24.43, which agrees with the theoretical analysis approximately. Figure 3 plots the electrical output spectrum of conventional scheme and the proposed scheme with third-order predistortion. Figure 3(a) shows that the carrier-to-intermodulation ratio (C/IM) is only

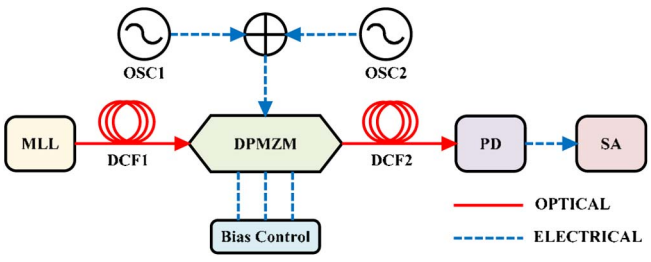

Fig. 2. Experimental setup of the proposed photonic time-stretched ADC based third-order predistortion (OSC, oscillator; SA, spectrum analyzer).

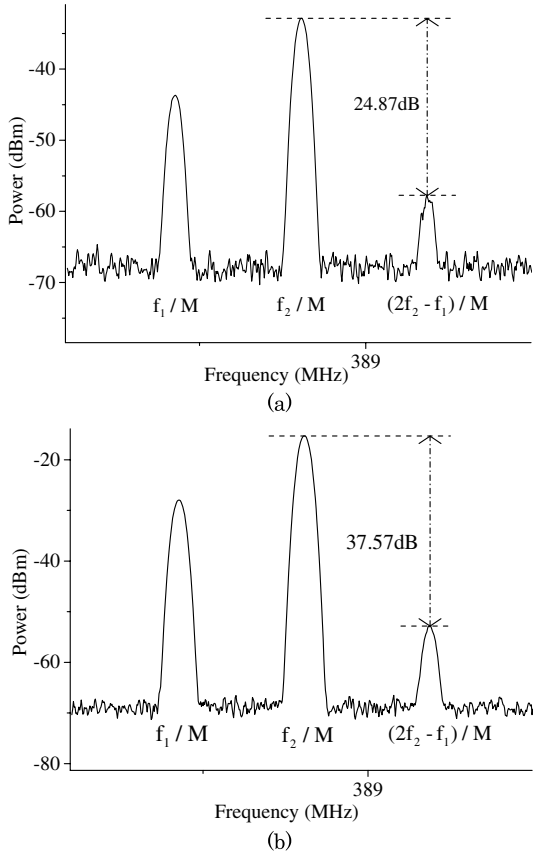

Fig. 3. (a) Electronic output spectrum for the conventional scheme without predistortion by using a common MZM. (b) Electronic output spectrum for the highly linearized scheme based on third-order predistortion by using DPMZM.

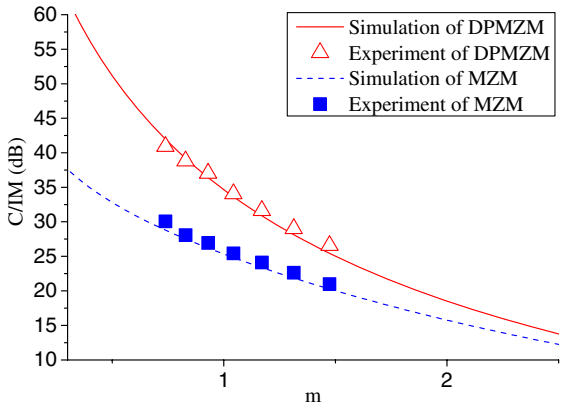

Fig. 4. Simulation and experimental results show the C/IM as a function of the modulation index m.

24.87 dB without predistortion, while the C/IM of the proposed scheme can be up to 37.57 dB as shown in Fig. 3(b), a 13 dB improvement in C/IM by predistortion compared with the conventional MZM.

Figure 4 shows the C/IM as a function of the modulation index m. The experimental results agree well with the simulation results, which prove theoretical the analysis in the last section. It can be seen in Fig. 4 that a rising modulation index m will result in performance degradation in both our proposed scheme and the conventional scheme. Nevertheless, our proposed scheme has better performance at the high power input region compared with the conventional one.

Figure 5 shows that the power of the fundamental and IMD3 of the stretched signal verifies with the power of the input electronic signal. The noise floor is calculated to be −154.73 dBm/Hz, by taking the thermal noise and the shot noise into consideration. It can be seen in Fig. 5(a) that the SFDR of the conventional scheme without predistortion is 69.20 dBm/Hz$^{2/3}$, while our linearized scheme with third-order predistortion has a SFDR of 95.15 dBm/Hz$^{2/3}$ as shown in Fig. 5(b). The difference of the SFDR of the two schemes is 25.95 dB, to prove our scheme has high linearity compared with the conventional one.

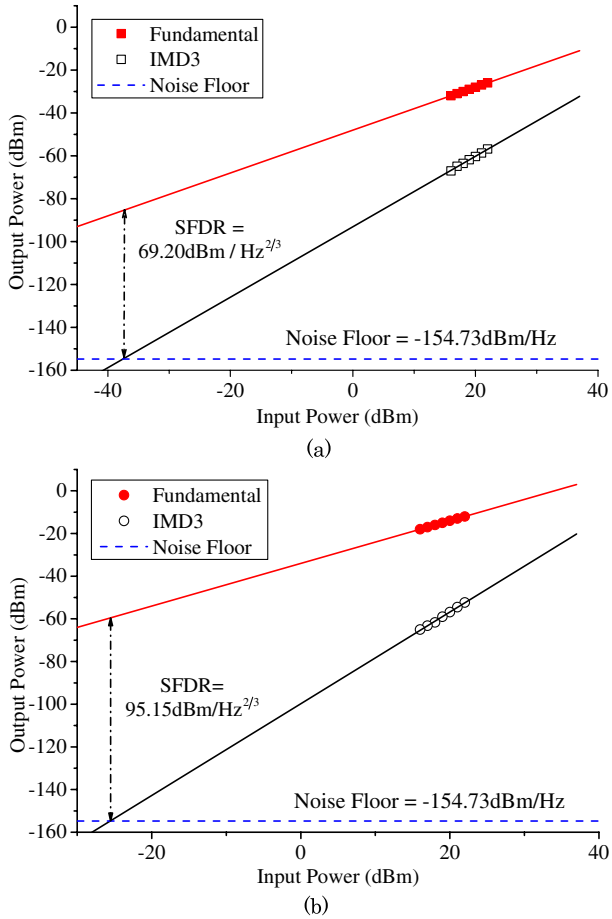

Fig. 5. Power of the stretched signal as a function of electronic input power for our proposed scheme and conventional scheme without predistortion. (a) Squares and lines represent the experimental data and linear fits to the fundamental and limiting IMD3 of common MZM scheme. (b) Circles and lines represent the experimental and linear fits to the fundamental and limiting IMD3 of the proposed DPMZM scheme.

Compared with other optical links, such as the linear radio-over-fiber (ROF) system, of which the SDFR can be above 100 dBm/Hz$^{2/3}$ [12], it seems that the SFDR of our highly linearized photonic time-stretched ADC is not high enough. However, we should notice that in the photonic time-stretched system, the amplitude of the signal is reduced by the stretch factor M, and this can reduce the SFDR of the photonic time-stretched ADC. So if the stretch factor M becomes smaller, a better SFDR than our experimental result can be obtained. However, a smaller M means a reduction of the input bandwidth, so there is a trade-off between the SFDR and the input bandwidth of the photonic time-stretched ADC.

4. CONCLUSION

A novel linearized scheme based on third-order predistortion by using an integrated DPMZM as a predistorter in a photonic time-stretched ADC is proposed in this paper. The experimental result shows that the SFDR of the proposed system is 95.15 dBm/Hz$^{2/3}$, about 26 dB improvement compared with that of the conventional one. The proposed linearized photonic time-stretched ADC features high efficiency and simplicity in structure. It has great potential applications in signal processing systems, such as in the radar and telecommunications areas.

ACKNOWLEDGMENTS

The work was supported by the National Basic Research Program of China (973 Program) (Grant No. 2012CB315703) and the Natural Science Foundation of China (Grant Nos. 61371029 and 60971060).

REFERENCES

1. R. H. Walden, “Analog-to-digital converter survey and analysis,” IEEE J. Sel. Areas Commun. **17**, 539–550 (1999).
2. R. Walden, “Analog-to-digital conversion in the early twenty-first century,” in *Wiley Encyclopedia of Computer Science and Engineering* (Wiley, 2008), pp. 126–138.
3. G. C. Valley, “Photonic analog-to-digital converters,” Opt. Express **15**, 1955–1982 (2007).
4. J. Capmany and D. Novak, “Microwave photonics combines two worlds,” Nat. Photonics **1**, 319–330 (2007).
5. Y. Han and B. Jalali, “Photonic time-stretched analog-to-digital converter: fundamental concepts and practical considerations,” J. Lightwave Technol. **21**, 3085–3103 (2003).
6. S. Gupta and B. Jalali, “2nd order distortion cancellation in photonic time stretch analog-to-digital converter,” in

Proceedings of IEEE Conference on Microwave Symposium Digest (Institute of Electrical and Electronics Engineers, 2007), pp. 229–232.
7. S. Gupta, G. C. Valley, and B. Jalali, "Distortion cancellation in time-stretch analog-to-digital converter," J. Lightwave Technol. **25**, 3716–3721 (2007).
8. H. S. Jang, H. T. Jeong, C. D. Kim, and I. S. Chang, "New predistortion method using phase modulation with envelope signal," in *Proceedings of IEEE Conference on Microwave Symposium Digest* (Institute of Electrical and Electronics Engineers, 2003), pp. 1339–1342.
9. G. C. Wilson, "Optimized predistortion of overmodulated Mach–Zehnder modulators with multicarrier input," IEEE Photon. Technol. Lett. **9**, 1535–1537 (1997).
10. Y. Tang, K. P. Ho, and W. Shieh, "Coherent optical OFDM transmitter design employing predistortion," IEEE Photon. Technol. Lett. **20**, 954–956 (2008).
11. R. W. Boyd, *Nonlinear Optics* (Academic, 2003).
12. B. Masella, B. Hraimel, and X. Zhang, "Enhanced spurious-free dynamic range using mixed polarization in optical single sideband Mach–Zehnder modulator," J. Lightwave Technol. **27**, 3034–3041 (2009).